

EXPERIMENTAL STUDY TO EVALUATE YIELDING POINT OF A REINFORCED CONCRETE BEAM WITH SLAB

Pranjal SATYA*¹, Tatsuya ASAI*², Masaomi TESHIGAWARA*³ and Ippei MARUYAMA*³

ABSTRACT

Several studies have been carried out to understand the performance of beam with slab specimen. The concept of effective width has been used in RC standards to evaluate the contribution of a slab to the beams in terms of stiffness and moment of resistance. The contribution of stiffness and moment capacity has to be quantified. A precise definition of yield deformation is very significant in the context of seismic loads and seismic performance of an RC structure. The yield point is characterized by significant energy absorption therefore energy absorption can be an important index to define yield point.

Keywords: RC beam-slab, Load-displacement, yield point, component contribution, energy absorption

1. INTRODUCTION

The yield point characterizes the seismic performance of a structure. As the yield point is characterized by significant energy absorption. Therefore, several studies are carried out to understand the bending behavior of the RC structural units such as a beam. Therefore load-displacement is a good index for measuring the seismic performance of the structures. Since the slab affects the bending performance of the beam, RC standards have provisions for the partial contribution of the slab^[1].

This study is focused on the bending performance of the RC beam with slab under static cyclic load. It focuses on the contribution of the slab to the bending behavior of the beam. Huge stubs are used to provide actual restraint conditions. In this study, firstly, load-displacement is studied, followed by crack patterns, rotation, and

displacement along with the height. The impact of the slab over beam performance is studied through its contribution to the stiffness and capacity. The yield point has been defined through energy absorption also.

2. EXPERIMENTAL OUTLINE

2.1. Specimen outline

The test specimen is a composite structure of two large beams, a sub-beam, and slab as represented in Fig 1. High strength rebars are used for large beams. The specimen was loaded after underwater curing of 100 days.

2.2. Loading arrangements

The specimen was loaded for 17 cycles with the first three cycles load controlled, and then the rest were displacement controlled. The loading cycle followed the following steps ± 10 kN, ± 20 kN, ± 30 kN, $\pm 1/2000$, $\pm 1/1000$, $\pm 1/400$ (2 cycles), $\pm 1/200$ (2 cycles), $\pm 1/133$ (2

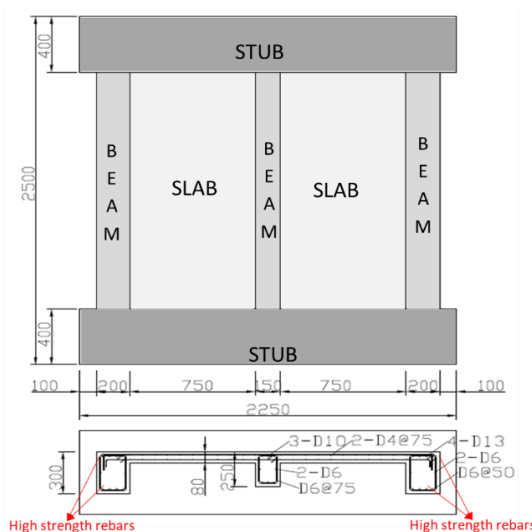


Fig. 1 Specimen outline

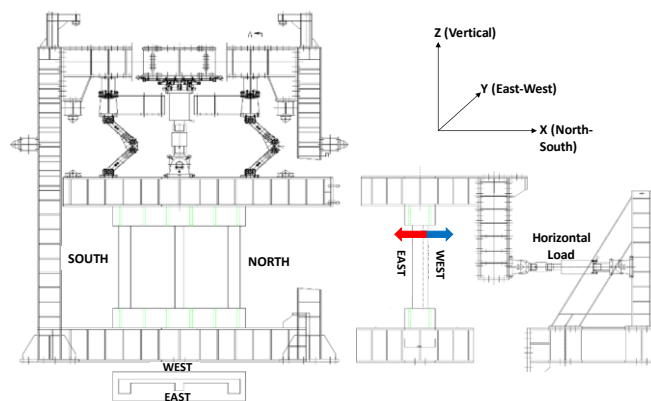


Fig. 2 Loading arrangements

*1 PhD. student., Graduate School of Environmental Studies, Nagoya University, JCI Student Member

*2 Assistant Professor, Graduate School of Environmental Studies, Nagoya University, JCI Member

*3 Professor, Graduate School of Environmental Studies, Nagoya University, JCI Member

cycles), $\pm 1/100$ (2 cycles), $\pm 1/50$ (2 cycles) and $\pm 1/25$ (2 cycles). The bottom stub is fixed for displacement in all directions and rotation about all directions. The top of the specimen is restrained for displacement in the x-direction and restrained for rotation about the y-axis, as shown in Fig. 2. In this study, positive loading is referred to as the load applied outwards (East to west) to the plane of the slab as represented by a blue arrow in Fig. 2. For positive loading slab at the bottom is in compression, and slab at the top is in tension and vice versa for negative loading.

2.3. Measurement Details

Moment distribution along the height varied linearly from the top (maximum +ve or -ve) to bottom (maximum +ve or -ve). Some strain gauges were attached at the top and bottom of the specimen, as shown by brown marks in Fig. 3. Displacement gauges shown by blue arrows in Fig. 3. were used to measure the vertical displacement on the east and west sides of the specimen. The displacement gauges measured the same vertical sections on both (east and west) sides of the large beam. These displacements are used to calculate the rotation and integrate it to obtain bending displacement of the specimen shown in Fig. 6a, and Fig. 6b. The straight line represents the vertical displacement measurement section in Fig. 6a, and Fig. 6b.

2.4. Material property

(1) Reinforcing materials

The material properties by direct tensile tests for the four types of rebar used are summarized in table 1.

Table 1 Reinforcement details

	Location	Steel type	f_y (MPa)
D4	Slab	SD345	357
D6	Stirrups	SD345	420
D10	Sub-beam	SD345	360
D13	Large beam	SD545	545

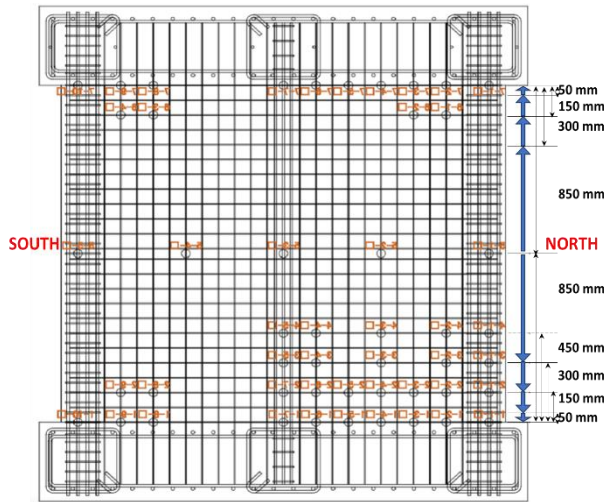


Fig. 3 Strain gauge and displacement gauge arrangements

(2) Concrete

The property test for concrete, which includes compressive strength, split tensile test, and fracture energy test, was carried at the time of loading test. The specimen used for property tests were as per RC standard. The compressive strength and tensile strength (at the age of 100 days), however, show deviation from 28-day strength (27 MPa) to be equal to 30 MPa and 2.5 MPa, respectively.

2.5. Load-displacement simplified calculation

The capacity of the specimen is calculated, assuming that both layers of rebar of the slab contribute to the total capacity when the slab is in tension, and the neutral axis is a straight line. The capacity at the crack, yield, and ultimate failure is evaluated as per AIJ standards^[1], as shown in the Eqs. 1, 2, 3, and 4. The capacity of the specimen when the west side is in tension includes the contribution of the large beam, sub-beam, and slab. When the west side is in compression, the capacity of the specimen is contributed only by the large beams and sub-beam. Stiffness degradation coefficient (α_y)^[1] is used for obtaining the effective stiffness of the specimen after cracking. The calculated load-displacement relationship is shown in Fig. 4 with the reddish-brown line.

$$\sigma_{cr} = 0.6\sqrt{f_{ck}} \quad (1)$$

$$M_{cr} = \sigma_{cr} \frac{I}{y} \quad (2)$$

$$M_y = \frac{7}{8} \times a_{st} \sigma_y \times d \quad (3)$$

$$M_u = 0.9 \times (a_{st} \sigma_y \times 1.1) \times d \quad (4)$$

Where σ_{cr} , f_{ck} , σ_y , I , y , M_{cr} , M_y , and M_u are the stress of concrete at crack characteristic strength of concrete, characteristic strength of steel, Inertia, depth of outermost fiber from the neutral axis, moment capacity at the crack, yield and at failure.

3. TEST RESULTS

3.1. Load-displacement relationship

The load-displacement relationship is represented in Fig. 4. The initial stiffness from test results and calculations based on AIJ standards comply with each

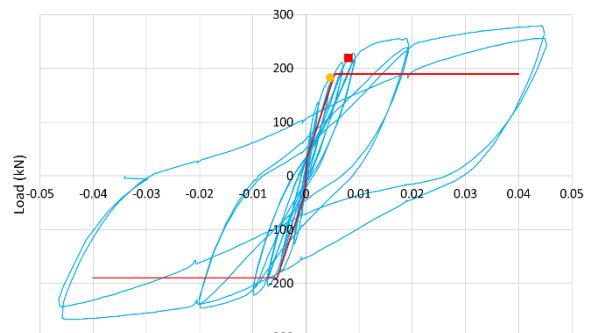


Fig. 4a Load-displacement relationship

other, as shown in Fig. 4b. The yielding of slab rebar started at 1/400, whereas large beam rebar (high strength rebar) yielding starts at 1/133. All the rebar yielded at 1/75. But the loading cycle of 1/75 was not

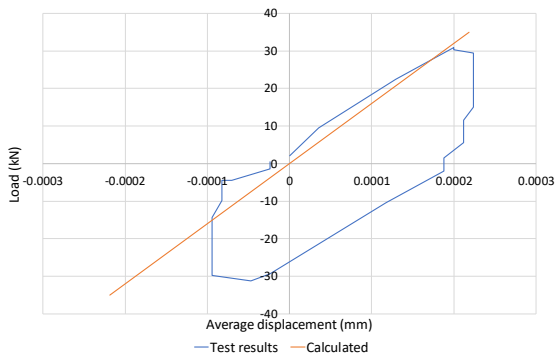


Fig. 4b Comparison of initial stiffness

considered during loading tests. The yield capacity from test results is comparatively higher in comparison to the calculated capacity. As per the calculation, the assumed neutral axis is close to the slab. But for loading test results, the neutral axis is at more distance for large beam as compared to the calculation. Hence, the capacity of a large beam increased, thereby also increasing the capacity of the specimen.

3.2. Crack patterns

The cracks observed are mainly bending cracks and are concentrated at the top and bottom of the specimen. Moments at top and bottom are maximum for any

applied horizontal load, as discussed in section 2.2. The cracks represented in Fig. 5 with blue and red color are cracks due to positive loading and negative loading respectively up to the loading cycle of 1/25. On the west side of the specimen the cracks for positive loading are concentrated on top while for negative loading at the bottom of the specimen. These cracks are because the surface is in tension which results in cracking. On the east side of the specimen cracks are observed at both ends of the specimen for positive and negative loadings. This mixed crack pattern is observed due to the shifting of the neutral axis into the slab. The depth of the neutral axis is such that the slab part on the east side of the specimen is in tension for both loading conditions. Therefore, cracks are observed for both positive loadings as well as negative loading. The crack patterns for the loading cycle of 1/25 are shown in Fig. 5. After yielding the cracks extend in length and expand in width with each loading cycle. Diagonal cracks were also observed for both loadings. It is due to bulging out of the slab. Cracks are observed up to a height of 2D, where D is the depth of beams.

3.3. Rotation along with the height and bending displacement

Vertical displacement was measured for the east side and west side of the specimens using displacement gauges as discussed in section 2.3. Segmental (local) rotation is obtained by dividing the difference of vertical displacements by horizontal distance between corresponding displacement gauges. The rotation of

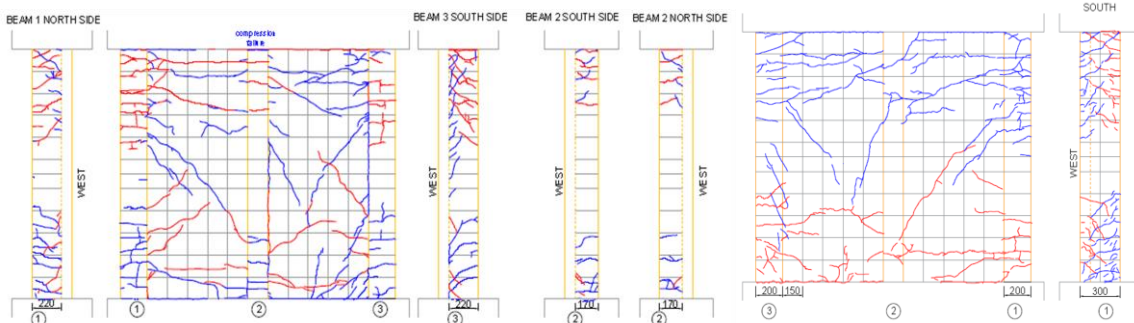


Fig. 5a Crack patterns (East side)

Fig. 5b Crack patterns (West side)

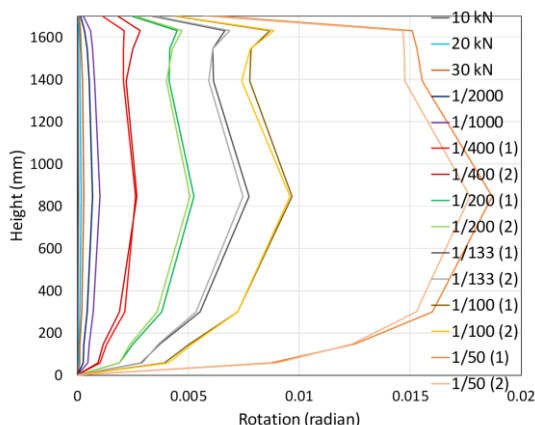


Fig. 6a Rotation along the height of the specimen

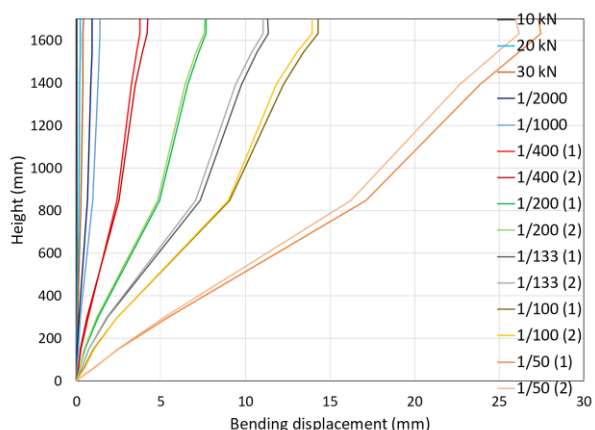


Fig. 6b Bending displacement along the height of the specimen

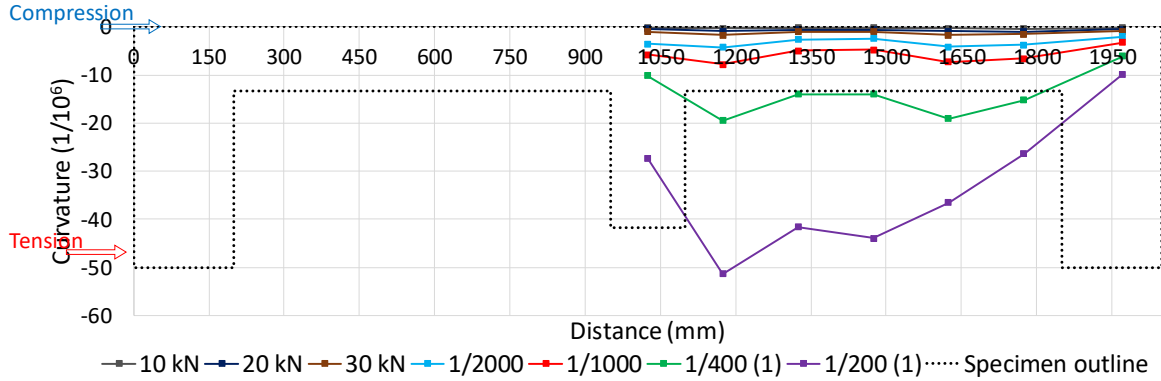


Fig. 7 Curvature distribution along width (slab in compression)

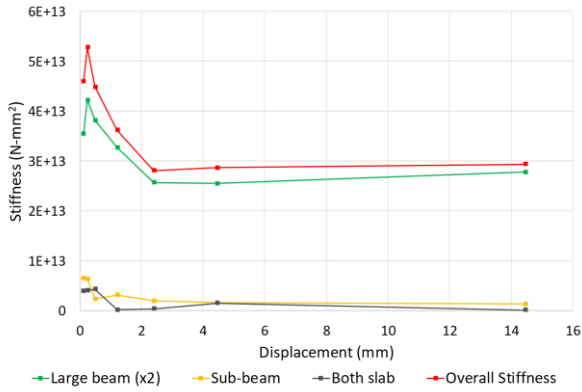


Fig. 8a Stiffness contribution (slab in tension)

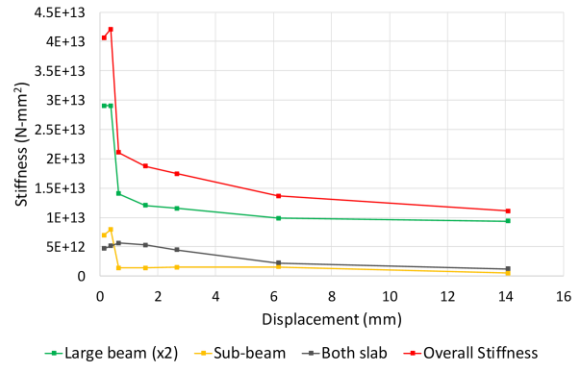


Fig. 8b Stiffness contribution (slab in compression)

specimen along with the height is shown in Fig. 6a. Bending displacement is obtained by integration of rotation along with the height assuming constant curvature for each segment. The bending displacement for each loading cycle is represented in Fig. 6b. The bending displacement calculated is about 83% of total horizontal displacement at the yielding of large beam rebar (11.34mm / 13.63mm). Therefore, the dominant displacement is bending displacement.

3.4. Curvature distribution along the width

The curvature distribution along the width of the specimen is represented in Fig. 7 for slab in compression, but this pattern is equally true for slab in tension also. It is observed that strain in slab rebars is higher as compared to that of beam rebars. These strain values from both sides of the specimen are used to calculate the curvature for any given section by the Eq. 5 shown below. The curvature distribution represented in Fig. 7 is for the bottom section of the specimen. It is evident from it that the curvature of the slab part is higher in comparison to the large beam. West side of the specimen will bend equally for slab and beam. The depth of slab is less, and one side of slab is in tension while other side is in compression. This implies that neutral axis lies within slab. Therefore, for same amount of rotation with lower depth result in higher curvature. The distribution pattern for curvature along the width of the specimen is similar for slab in tension as well as a slab in compression.

$$Curvature (\phi) = \frac{\varepsilon_1 - \varepsilon_2}{d_s} \quad (5)$$

Where, ε_1 , ε_2 and d_s are strain of rebars on both sides and distance between the rebars.

4. CONTRIBUTION OF EACH COMPONENT

4.1. Stiffness contribution

The specimen has not a regular cross-section i.e. it is not a plane rectangular beam therefore total stiffness is the sum of the stiffness contribution of each component (large beams, sub-beam and slab). The stiffness is calculated through the following steps. Given data: strain values (ε_1 & ε_2) on both sides of the specimen (west side and east side).

$$\text{Step 1} \quad \text{Neutral axis} = \frac{\varepsilon_1 \times d}{\varepsilon_1 + \varepsilon_2} \quad (6)$$

$$\text{Step 2} \quad I_c = I_a + I_b \quad (7)$$

$$I_{a \text{ or } b} = \frac{bh^3}{12} + A \times \left(\frac{h}{2}\right)^2 \quad (8)$$

$$I_s = n \times \left(\frac{\pi D^4}{64} + a_{st} \times (NA - cover)^2\right) \quad (9)$$

$$\text{Step 3} \quad \text{Total stiffness } (EI) = E_c I_c + E_s I_s \quad (10)$$

Where, ε_1 and ε_2 strain values of rebar on both sides of the specimen, d is effective depth, b =width of the section, h is the depth of the assumed section above or below the

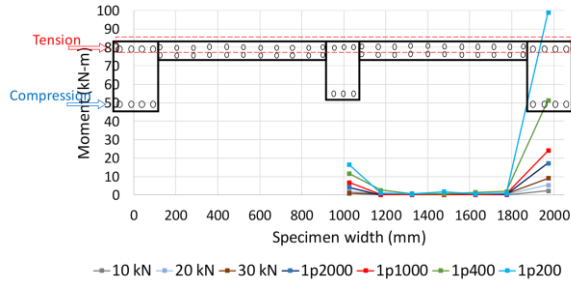


Fig. 9a Moment distribution (slab in tension)

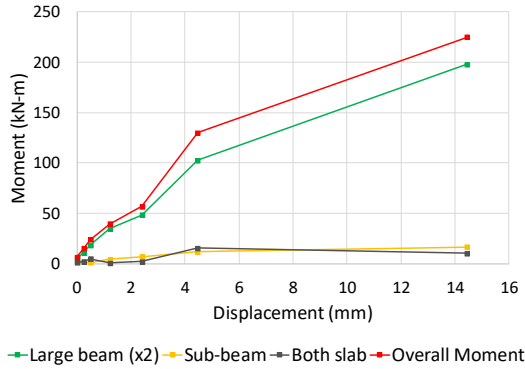


Fig. 10a Moment contribution (slab in tension)

neutral axis, A is the area of section = bh , I_c , I_a , I_b , and I_s are the second moment of area about a neutral axis for concrete sections, above and below the neutral axis and rebars. E_c and E_s are Young's modulus of concrete and steel, respectively. NA is the depth of neutral axis, a_{st} is an area of one rebar, the cover represents nominal concrete cover to rebars. $(NA - \text{cover})$ represents the distance of rebar from the neutral axis.

The contribution of stiffness from each component is represented in Fig. 8a, and Fig. 8b for slab in tension and compression, respectively. The contribution of concrete in tension zone after cracking is neglected in this stiffness calculation. Effective stiffness for rebars after yielding is obtained as secant stiffness at that strain from the stress-strain relationship of the given rebars. Stiffness of the specimen and its component is represented in Fig. 8a, and Fig. 8b for slab in tension and compression, respectively. Since the depth of the neutral axis calculated from Eq. 6 is higher for slab in tension, the stiffness also becomes higher. Stiffness represented for the large beam is the sum of the stiffness of two large beams. Stiffness of slab is the sum of the stiffness of both slabs.

4.2. Moment contribution

The contribution of each component refers to the share of the capacity of beams and slab to the total capacity of the specimen. The individual capacity as per calculation for the large beam is 125 kN-m, for sub-beam is 13.9 kN-m, and 183.8 kN-m is the yield capacity of the specimen. Therefore, the contribution of the slab is 44.9 kN-m. The sectional contribution from the specimen is represented in Fig. 9a, and Fig. 9b. Strain values are used to obtain the contribution of each

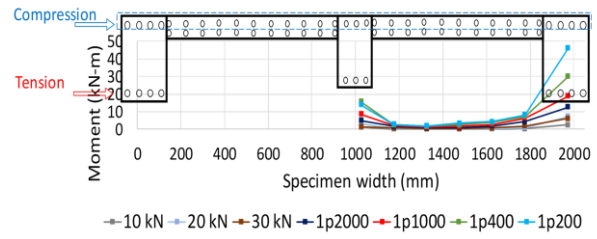


Fig. 9b Moment distribution (slab in compression)

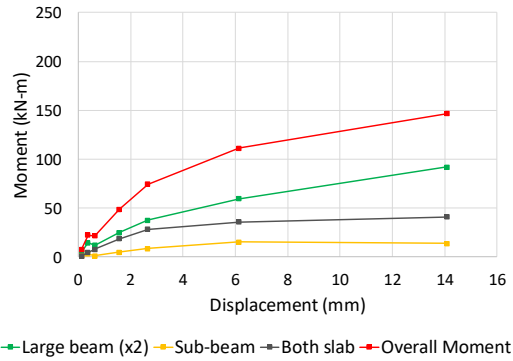


Fig. 10b Moment contribution (slab in compression)

component. Firstly, strain from both sides of the specimen is used to calculate curvature as described in section 3.4, the depth of the neutral axis and stiffness is calculated as discussed in section 4.1. The moment capacity is obtained as the product of stiffness and curvature as shown in the Eq. 11 below.

$$Moment (M) = EI\phi \quad (11)$$

Where, EI and ϕ are stiffness and curvature.

The contribution of each component i.e. large beams, sub-beam and slab is shown in Fig. 10a and Fig. 10b. It is observed that for slab in compression significant contribution from each component is obtained. But for slab in tension almost all the capacity is due to the large beams (approximately 90%). The calculated load capacity of the specimen is compared with the test results and is represented in Fig. 11. For higher displacements the calculated load is higher. It is

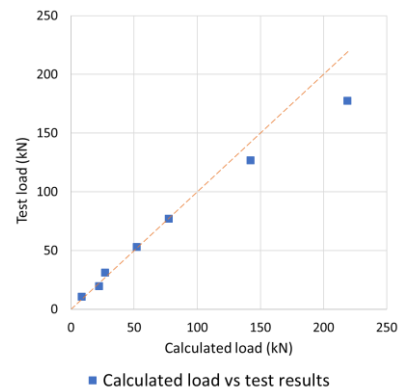


Fig. 11 Test load vs calculated load

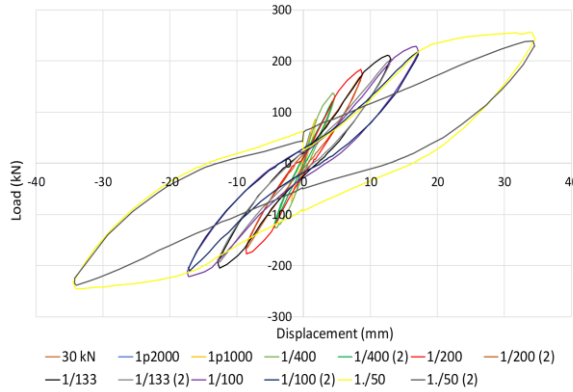


Fig. 12a Energy absorption

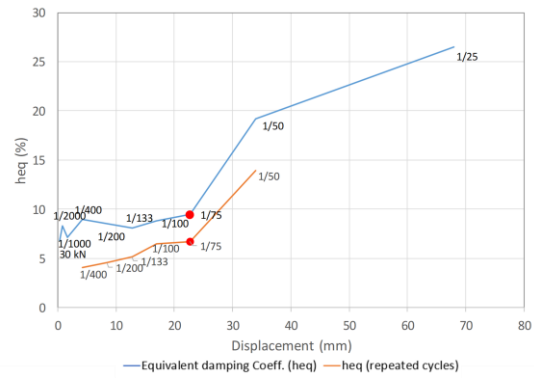


Fig. 12b Equivalent damping coeff. (heq)

due to the fact that the Young's modulus for concrete is not modified for higher displacements. Young's modulus of concrete for higher displacements is reduced considerably therefore the calculated capacity will be lower.

5. ENERGY ABSORPTION

The energy imparted to any structure is dissipated within the structure. The dissipation of energy is an important characteristic that defines structural performance under seismic loading. Fig. 12a, and Fig. 12b represents the energy absorption and equivalent damping coefficient, respectively. As it is observed that there is no significant change up to a cycle of 1/100. But from the test results, it is observed that all rebars yielded at a displacement of exactly at 1/75. From 1/100 to 1/75, no unusual event is observed, and load increases linearly with displacement up to this point. So, it can be concluded that the yielding of the specimen is between 1/100 and 1/50. The slab rebars and sub-beam rebar started yielded at 1/133. Large beam rebars yielded at 1/100. Similar patterns are observed for repeated cycles. Therefore, to define the yielding point of the specimen yielding of the large beam should be focused.

6. CONCLUSION

The conclusion drawn from this study includes crack patterns are affected by the depth of the neutral axis, which can result in mixed crack patterns. The dominant displacement is bending displacement, with a majority of bending cracks. The depth of the neutral axis also defines the contribution of components to stiffness and capacity. A major contribution is of the large beam for stiffness and capacity. For slab in tension, slab affects the stress distribution, thereby increasing the capacity.

While for slab in compression, the negligible effect can be observed for stress distribution from slab to beam. This means that for slab in tension, all the compressive stress is taken by large beams. The significant change in energy absorption observed after the yielding of large beam rebars. Therefore, to obtain the yielding point of the specimen, large beams shall be focused.

ACKNOWLEDGMENT

This research is partially performed in the project funded by the Ministry of Land, Infrastructure, Transportation and Tourism (S30). Authors also express their gratefulness towards the laboratory members Nagoya University and Yamaguchi University students; without them, this study could not have been possible.

REFERENCES

- [1] Architectural Institute in Japan, "AIJ standard for Structural Calculation of Reinforced Concrete Structures," 2018
- [2] Lu, X., et al., "Experimental investigation of RC beam-slab substructures under progressive collapse subject to an edge column removal scenario," *Engineering Structures*, 149 (2017) 91-103
- [3] Sasano, H., et al., "Impact of Drying on Structural Performance of Reinforced Concrete Shear Walls," *Journal of Advanced Concrete Technology*, Vol.16, No.5, 2018, pp. 210-232
- [4] Hameed, R., et al., "Behavior of Reinforced Fibrous Concrete Beams under Reverse Cyclic Loading," *Pak. J. Engg. & Appl. Sci.* Vol. 9, Jul. 2011 (p. 1-12)